

# Electroless Metalization of Halloysite, a Hollow Cylindrical 1:1 Aluminosilicate of Submicron Diameter

Subhash Baral,<sup>\*,†</sup> Susan Brandow,<sup>‡</sup> and Bruce P. Gaber<sup>§</sup>

Geo-Centers Inc. 10903 Indian Head Hwy., Ft. Washington, Maryland 20744; Department of Chemistry, University of Colorado, Boulder, Colorado 80309; and Center for Bio/Molecular Science and Engineering, Code 6900, Naval Research Laboratory, Washington D.C. 20375-5000

Received February 25, 1993. Revised Manuscript Received June 14, 1993

A new kind of cermet has been produced by electroless metalization of the mineral halloysite. The aluminosilicate particles of approximately 1- $\mu$ m length and 100-nm diameter were coated with roughly 20-nm-thick microcrystalline nickel film. Electron and atomic force microscopy, thermogravimetry, and electron and X-ray diffraction studies have been used to characterize the original halloysite and the metalized product. Potential applications of these novel cermet particles are delineated.

## Introduction

Concentrated aqueous suspensions of clays are widely used as precursors in the manufacturing of conventional and advanced ceramic materials.<sup>1,2</sup> Recently clay minerals have also found potential use as fillers (up to 60%) in composites derived from organic polymeric materials such as resins, rubbers, and plastics.<sup>3</sup> Surface modifications of superfine clay particles via chemical methods have been used to alter particle-particle or particle-matrix interactions in a controlled manner to improve the mechanical and other materials properties of these ceramic or organic composite materials.<sup>4</sup>

Halloysite (composition:  $\text{Al}_2\text{Si}_2\text{O}_5(\text{OH})_4 \cdot 2\text{H}_2\text{O}$ , 1:1 layer aluminosilicate), a clay mineral, occurs frequently in nature as ultramicroscopic hollow cylinders. [A mismatch in the periodicity between the oxygen sharing tetrahedral  $\text{SiO}_4$  sheets and adjacent octahedral  $\text{AlO}_6$  sheets in the 1:1 layer structure of halloysite results in curvature (roll-up) giving these clay particles a hollow cylindrical shape.<sup>5</sup>] We have used these micron-sized cylinders of submicron diameter as templates for metal deposition with the ultimate goal of producing cermet particles with structure consisting of a ceramic cylinder coated with concentric metal film(s). We believe that metalized structures such as this may be used to produce low-cost clay-based advanced composite materials, in which the metal film serves<sup>2</sup> as an interphase, as a vehicle for orientation and organization, and as a modifier of dielectric properties. These composite ma-

terials have potential structural, electromagnetic shielding, and microwave applications. The presence of the hollow cylindrical cavity in ferromagnetic metal coated halloysite particles may also be exploited for targeted controlled release, waste scavenger, and sensor applications.

Since halloysite particles are electrically insulating and are of microscopic (colloidal) dimensions, conventional film deposition methods such as vapor deposition, sputtering, molecular beam deposition, and electrolytic deposition could not be used to uniformly coat individual halloysite particles. We have used a chemical technique commonly known as electroless plating<sup>6</sup> to build a thin film of nickel metal on the surface of halloysite particles. The metalization process and the characterization of the metalized halloysite are described in the present paper.

## Experimental Procedures:

**Chemical Reagents.** Halloysite (Bedford, Indiana) was obtained as an off-white coarse powder from Ward's Natural Science Establishment Inc (Rochester, NY). Palladium chloride and stannous chloride were obtained from Aldrich Chemical Co. (Milwaukee, WI). The Niposit468 electroless plating bath was obtained from Shipley Co (Newton, MA). All other reagents were of analytical grade. Water was twice distilled in an all-glass still.

**Purification of Halloysite.** The crude halloysite mineral (approximately 100 g) was ground with water to a thin slurry which was then screened through a 125- $\mu$ m size sieve to remove grits and stones. The slurry was suspended in 2 L of water. Material remaining in dispersion after 5 min was collected by centrifugation (the solid which had precipitated was recycled for further grinding). The centrifuged solid paste was shaken with 0.5 M tetrasodium ethylenediamine tetraacetate (EDTA) solution in water for 24 h. Subsequent centrifugation of the dispersion produced an almost white wet solid which was further ground in an agate mortar and pestle. Scanning electron micrographs of the ground solid indicate that it consists of cylindrical halloysite particles together with some uncharacteristic shaped material. The halloysite particles were subsequently concentrated by fractionation through redispersions and selective centrifugations. The fractionation process was monitored by SEM. The halloysite enriched fraction was air-dried at room temperature to a pure white powder (yield 8-10% based on crude mineral).

\* Corresponding author. Present address: Anne Arundel County Police Department, 8495 Veterans Hwy, Millersville, MD 21108.

<sup>†</sup> Geo-Centers, Inc.

<sup>‡</sup> University of Colorado.

<sup>§</sup> Center for Bio/Molecular Science and Engineering.

(1) (a) Wilson, H. *Ceramics-Clay Technology*; McGraw-Hill Book Co.: New York, 1987. (b) Brook, R. J., Ed. *Concise Encyclopedia of Advanced Ceramic Materials*; Pergamon Press: Berlin, 1991; pp 324-357. (2) Schwartz, M. M. *Composite materials Handbook*; McGraw-Hill Book Co.: New York, 1983.

(3) (a) Wilcox, J. R. Controlling Flow Properties with Fillers. *Proc. Soc. Plastics Inc.* 1954, 9, Sect. 27. (b) Plueddemann, E. P. *Silane Coupling Agents*; Plenum Press: New York, 1991.

(4) (a) Clark, N. O.; Parker, T. W. British Patent 630,418, 1949. (b) Carter, L. W.; Hendricks, J. C.; Bolley, D. S. U.S. Patent 2,531,396, 1950. (c) Oya, A.; Kizu, K.; Otani, S. *Appl. Clay Sci.* 1988, 3, 205-207.

(5) (a) Bates, T. F.; Hildebrand, F. A.; Swineford, A. *Am. Mineral.* 1950, 6, 237-248; 1959, 35, 463-484. (b) Bates, T. F. *Am. Mineral.* 1959, 44, 78-114. (c) Churchman, G. J.; Carr, R. M. *Clays Clay Miner.* 1975, 23, 382-388.

(6) (a) Lukes, R. *Plating* 1964, 51, 1066. (b) Shipley, C. R. Jr. *Plating Surf. Finishing* 1984, 71, 92. (c) Cohen, R. L.; Meek, R. L.; West, K. W. *Plating* 1976, 63, 52.

Although conventional purification of clay minerals involves a slightly different procedure involving Calgon (sodium metaphosphate),<sup>7</sup> we found the EDTA treatment described above to be easier and importantly less interfering with subsequent catalyzation and metalization steps.

**Catalyzation of Halloysite.** The surface of the halloysite particles was activated toward electrodeless plating by a conventional method involving successive treatments with acidic palladium chloride and stannous chloride solutions.<sup>8</sup> Approximately 50–75 mg of purified halloysite powder was treated in the following manner:

- (1) Dispersed by vortexing with 2 mL of 0.05 M PdCl<sub>2</sub> solution at pH 1.0 (0.1 M HCl) for 2 min and then intermittently vortexed for another 10 min.
- (2) Centrifuged to discard the supernatant.
- (3) Washed twice with 0.1 M hydrochloric acid solution (by vortexing and centrifugation).
- (4) Vortexed with 2 mL of 0.1 M SnCl<sub>2</sub> solution in 0.5 M HCl for 2 min and then intermittently vortexed for another 10 min.
- (5) Centrifuged to discard the supernatant.
- (6) Washed twice with 0.1 M hydrochloric acid solution.
- (7) Steps 1–6 were repeated.
- (8) Step 1 was repeated.
- (9) Centrifuged to discard the supernatant.
- (10) Washed twice with water.

The light brown solid obtained at this point was subjected to immediate metalization. (On standing the catalyzed product slowly turns inactive in 4–6 h.)

**Metalization.** The activated halloysite was dispersed in 5 mL of water at 65 °C. The dispersion was mixed with 10 mL of Niposit468 plating bath at 65 °C. In about 5 min the mixture turns black and hydrogen bubbles start forming. The plating was continued at 65 °C with occasional vortexing to keep the halloysite particles well dispersed. After about 15 min another 10 mL of Niposit468 bath was added to the plating mixture. The plating was continued for an additional 60–80 min at 65 °C without disturbance. During this period the hydrogen evolution slowly dwindled and black metalized particles started to settle at the bottom. The supernatant plating bath was then siphoned off and the nickel-coated halloysite particles were washed with three 10-mL portions of water and two 20-mL portions of dry acetone. The nickel coated particles were stored under dry acetone.

**Characterization.** SEM micrographs were obtained over a range of magnifications after drying a drop of sample in aqueous suspension on an SEM stage. The solid residue was examined over random areas in a DISIDS-130 scanning electron microscope using a 6–10-keV electron beam. The energy-dispersion X-ray analysis (EDX) was done on the scattered beam with a Kevex 5100 detector attached to Kevex Analyst 8000 to determine the elemental composition within a penetration depth (of the electron beam) of about 5–10 nm from the surface of the particles.

Transmission electron microscopic examinations were performed after drying an aqueous suspension of the sample on a formvar film-coated copper grid and examining the residue (without staining) in a Zeiss EM-10 transmission electron microscope using a 50-keV electron beam. Selected area electron diffraction patterns as well as micrographs were also recorded in a JEOL 200CX transmission electron microscope using a 200-keV electron beam. The nickel-coated halloysite samples were also embedded in an epoxy matrix during sample preparations. The embedding was done by mixing a suspension of metalized halloysite in acetone with a very slow curing epoxy resin–hardener combination. The acetone was allowed to slowly evaporate in air at room temperature for about 48 h. The epoxy was then cured at 60 °C for 12 h (sometimes in the presence of a magnetic field). The composite was cut into 30–40-nm thin sections with a diamond ultramicrotome knife and examined by TEM and AFM techniques.

Atomic force microscopy (AFM) micrographs of the samples were taken using a commercial Nanoscope III AFM (Digital Instruments) equipped with microfabricated silicon nitride

cantilevers (Digital Instruments). Recently, successful AFM imaging of clay materials has been reported in the literature.<sup>9</sup> We have imaged both the untreated surface of a halloysite sample in addition to samples of metalized and purified nonmetalized halloysite embedded in epoxy resin.

The thermogravimetric analysis was done with a Perkin-Elmer TGA-7 instrument. A small amount of sample (typically 10–15 mg) was heated on a platinum crucible in nitrogen atmosphere at a rate of 5 or 10 °C/min to a final temperature of 900 °C. The weight change was recorded with a sensitive electrobalance.

The X-ray diffraction patterns were recorded in a Rigaku DMXAB X-ray diffractometer in the  $\theta$ - $2\theta$  mode using Cu K $\alpha$  radiation. Samples for diffraction measurements were prepared by spreading a thin slurry in water or acetone on a highly polished silicon wafer and subsequent air-drying.

The amount of nickel metal in the nickel coated halloysite samples was determined by standard gravimetric procedure. The nickel metal was brought into solution by treating the nickel-coated halloysite with dilute hydrochloric acid and subsequently was precipitated as nickel bisdimethylglyoxime complex, which was dried and weighed.

## Results and Discussions

Our preliminary experiments had indicated that halloysite purified by conventional Calgon treatment<sup>7</sup> does not metalize very well. A thicker, more uniform nickel film deposition was obtained with halloysite purified by the EDTA procedure. It seems that the Calgon treatment leaves some surface contamination which interferes with the catalyzation process. Since EDTA has not been used in the past for clay purification, we spent some efforts in characterizing the purified product. The specific gravity of the purified halloysite was found to be 2.5–2.6 (determined by centrifuging the halloysite particles in bromoform–methanol mixtures of various known specific gravities). This value is in accord with that reported (2.5) for pure halloysite.<sup>10</sup> Determination of elemental composition by EDX method showed the atomic ratio of Si:Al to be close to 1:1 as expected from an 1:1 aluminosilicate.<sup>11</sup> [EDX analysis of several purified halloysite fractions showed the average atomic composition to be Al 47.5%, Si 52.1%, and Fe 0.3% (normalized to 100% for all elements detected, except oxygen).] The morphology of purified halloysite particles was found by scanning electron microscopy to consist mostly of isolated (and also some clumped) cylinders of 80–100 nm in diameter and about a micrometer in length. This is consistent with the known morphology of halloysite derived by diagenesis of crystalline minerals such as feldspars or micas.<sup>11</sup> An AFM scan (1.6  $\mu\text{m} \times 1.6 \mu\text{m}$ ) of halloysite particles embedded in an epoxy surface is shown in Figure 1. The image revealed several isolated well-formed cylindrical structures. The average height of the cylinders was approximately 60 nm, indicating that the structures are significantly buried in epoxy. Widths ranging from 90 to 120 nm were measured, while the lengths of the cylinders were found to vary widely. [AFM micrographs (not shown) of the surface of a crude, untreated sample of halloysite mineral reveal several cylinders of comparable dimension. This strongly indicates that the purifying and embedding process does not significantly alter the morphology of halloysite particles.] Cylinders viewed end-on appeared

(9) Hartman, H.; Sposito, G.; Yang, A.; Manne, S.; Gould, S. A. C.; Hansma, P. K. *Clays Clay Mineral.* 1990, 38, 337–342.

(10) Loughnan, F. C. *Am. Mineral.* 1957, 42, 393–398.

(11) Newman, A. C. D.; Brown, G. *Chemistry of clays and clay minerals*; Mineralogical Society Monograph, No. 6, Newman, A. C. D. Ed.; Longman Science and Technical: Essex, England, 1987; pp 1–128.

(7) Churchman, G. J.; Gilkes, R. J. *Clay Minerals* 1989, 24, 579–590.

(8) (a) Pearlstein, F. *Met. Finishing* 1955, Aug, 59–61. (b) Cohen, R. L.; Meek, R. L. *J. Colloid Interface Sci.* 1976, 55, 156–162. (c) Schlesinger, M.; Kisel, J. *J. Electrochem. Soc.* 1989, 136, 1658–1661.

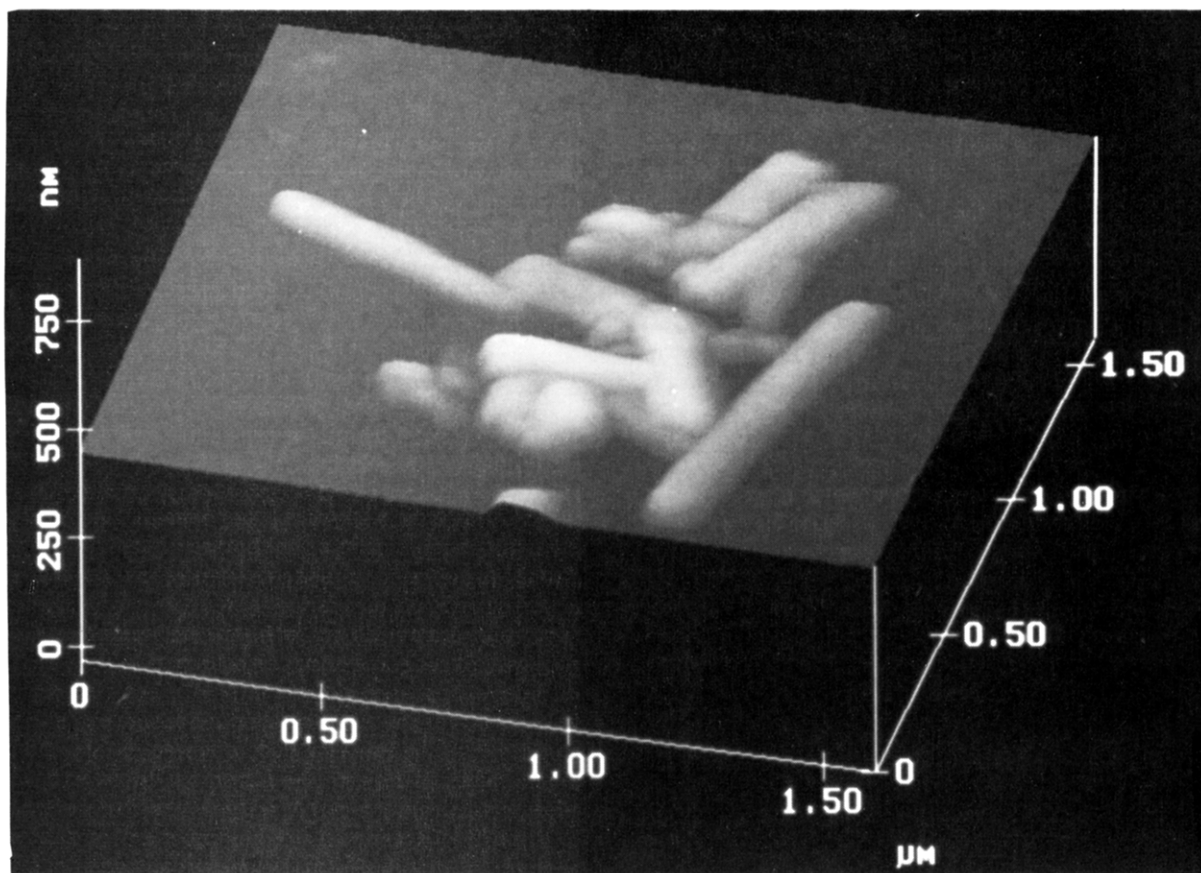


**Figure 1.** A  $1.6\ \mu\text{m} \times 1.6\ \mu\text{m}$  AFM scan of purified halloysite particles embedded in an epoxy resin matrix. Images of several halloysite particles are seen.

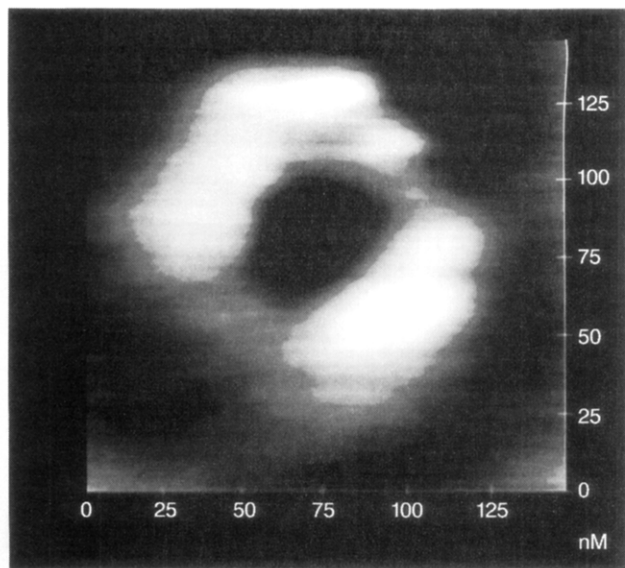


**Figure 2.** A  $150\ \text{nm} \times 150\ \text{nm}$  AFM scan showing a cross-sectional view of an exposed halloysite cylinder. The sample has been plasma etched to remove some of the epoxy from the tube's interior and from around the outside edges.

to contain epoxy inside. To remove epoxy around the tube edges a sample was plasma etched for 15 s. Figure 2 is a  $150\ \text{nm} \times 150\ \text{nm}$  AFM scan showing a cross-sectional view of the exposed cylinder after plasma etching. Although from the image the inner diameter of the tube appears to be approximately 40 nm, the resolution is limited by the aspect ratio of the AFM tip and subsequent convolution of the AFM tip shape in the image. However, the AFM micrograph in Figure 2 strongly suggests that

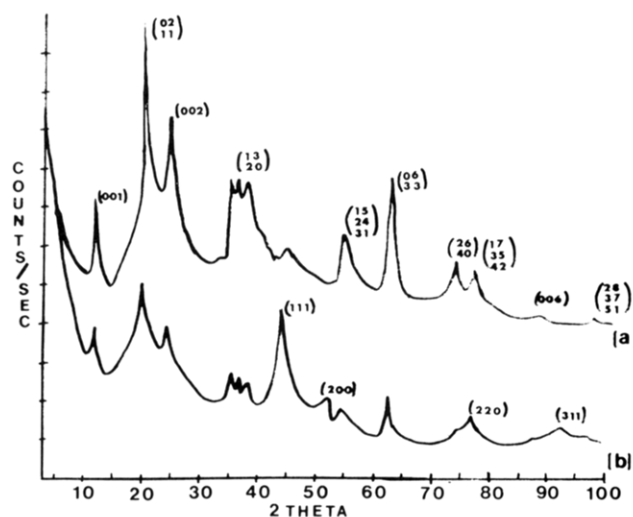


**Figure 3.** (a) X-ray powder diffraction pattern of purified halloysite. The diffraction peaks are indexed. (b) X-ray powder diffraction pattern of electroless nickel coated halloysite. Only the indexes of reflections originating from nickel are shown. The reflections originating from halloysite are the same as in Figure 3a.

the halloysite particles are open ended and hollow.

The X-ray powder diffraction pattern (Figure 3a) indicates that the purified halloysite is the partially dehydrated form or metahalloysite (also known as halloysite-7A) with an interlayer or basal spacing of 0.74 nm.<sup>12,13</sup> No peak was found at  $2\theta$  around  $9^\circ$  corresponding to an interlayer spacing (1 nm) of fully hydrated halloysite (halloysite-10A).<sup>12</sup> The various diffraction peaks in Figure 3a have been indexed as  $(00l)$  and  $(hk)$ . The  $(hk)$  peaks

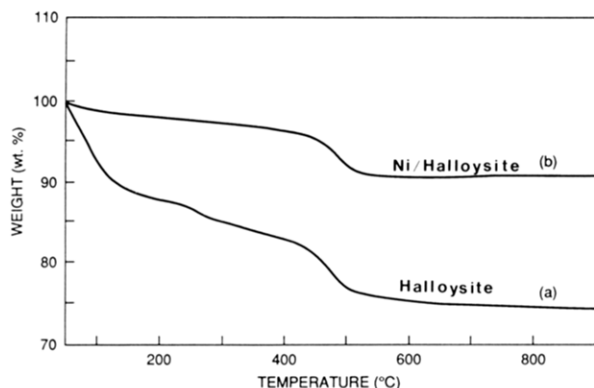


**Figure 4.** (a) Thermogravimetric analysis of purified halloysite. Sample weight was 15.457 mg. Heating rate was 5 °C/min. Nitrogen atmosphere. (b) Thermogravimetric analysis of electroless nickel coated halloysite. Sample weight was 12.847 mg. Other conditions are the same as in (a).

arise from a two-dimensional intralayer periodicity. No (*hkl*) peaks were observed. This powder pattern is entirely in accord with the results reported earlier.<sup>13</sup>

Thermogravimetric analysis on an air-dried sample is shown in Figure 4a. About 12% weight loss occurs between 50 and 135 °C, followed by another 1–2% weight loss between 230 and 350 °C. Finally a 10% weight loss occurs between 390 and 525 °C. The TGA curves are very similar to those reported earlier on standard samples of halloysite<sup>14</sup> except for the very small loss between 230 and 350 °C, which may be due to residual ferric oxide hydrate.<sup>15</sup> Removal of two water molecules from the hydrated compound  $\text{Al}_2\text{Si}_2\text{O}_5(\text{OH})_4 \cdot 2\text{H}_2\text{O}$  corresponds to a 14% weight loss. Thus, in the temperature range 50–135 °C, presumably two loosely bound water molecules (interlayer water) are lost, while between 390 and 525 °C the structural water (intralayer water present in the form of four hydroxy groups) was lost.<sup>14</sup> A halloysite sample dehydrated by heating at 500 °C for 10 h has been found by SEM to have identical cylindrical morphology as the original halloysite. Therefore, removal of structural water at 500 °C does not seem to alter the particle morphology.

The electroless plating process requires an initial sensitization (toward plating) of the surface to be plated.<sup>5</sup> In the present work, this has been accomplished by successive treatment of the halloysite particles with an acidic palladium chloride solution and an acidic stannous chloride solution.<sup>8,16</sup> Such treatment results in the formation of small palladium metal particles on the substrate surface which act as the catalyst for metal ion reduction.<sup>6,16</sup> The plating was done with Shipley Niposit 468 nickel plating bath, which deposits 99.9% pure ferromagnetic nickel metal of high electrical conductivity.<sup>17</sup>

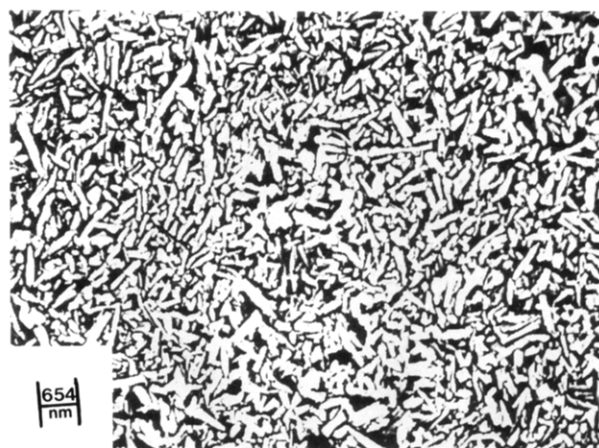


**Figure 5.** SEM micrographs of electroless nickel-plated halloysite particles. The sample was dried from acetone on an SEM stage before the micrograph was taken.

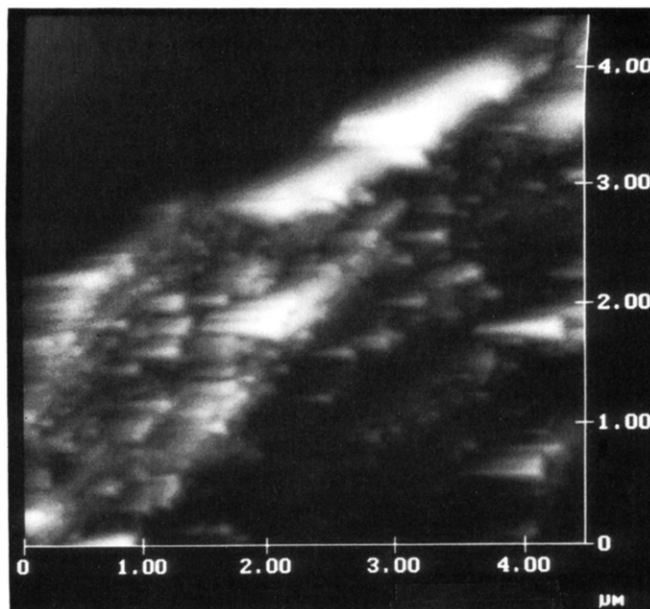


**Figure 6.** A 4.5 μm × 4.5 μm AFM scan of an aligned composite of nickel plated halloysite particles embedded in epoxy. The ferromagnetic particles were aligned with a small magnetic field (approximately 300 G) during the embedding process.

An SEM micrograph of the nickel-plated halloysite particles is shown in Figure 5. The absence of charging of the sample in the electron beam suggests the presence of a conductive metal film on the halloysite particles. Elemental analysis by EDX indicates the presence of 95.5 atom % of nickel on the surface (i.e., within a depth of 5–10 nm) of the nickel-coated halloysite particles. This result strongly suggests that the surface of halloysite particles is almost completely covered with nickel metal. Gravimetric determination of the nickel content of several different batches of plated samples indicated the presence of 35–45 wt % of nickel in these materials.

The nickel-coated halloysite particles are strongly ferromagnetic. They are attracted to and aligned by the presence of a magnetic field. Composite materials in which the nickel-coated halloysite particles are oriented parallel to each other can be obtained by dispersing the particles

(12) (a) Sudo, T.; Takahashi, H. *Clays Clay Miner.* **1956**, *4*, 67–79. (b) Anand, R. R.; Gilkes, R. J.; Armitage, T. M.; Hillyer, J. W. *Clays Clay Miner.* **1985**, *33*, 31–43.

(13) (a) Brindley, G. W. *The X-ray identification and crystal structures of clay minerals*; Brown, G., Ed.; Mineralogical Society: London, 1961; pp 51–131. (b) Mitra, G. B.; Bhattacharyya, S. *Acta Crystallogr.* **1975**, *B31*, 2851–2857. (c) Brindley, G. W. *Crystal Structures of Clay Minerals and Their X-ray identification*; Brindley, G. W., Brown, G. Eds.; Mineralogical Society: London, 1980; pp 126–197.

(14) (a) Weber, J. N.; Roy, R. *Am. Mineral.* **1965**, *50*, 1038–1045. (b) Churchman, G. J.; Carr, R. M. *Am. Mineral.* **1972**, *57*, 914–923. (c) Minato, H. *Thermochim. Acta* **1988**, *135*, 279–283. (d) Palomba, M.; Porcu, R. *J. Thermal Anal.* **1988**, *34*, 711–722.

(15) Posnjak, E.; Merwin, H. E. *Am. J. Sci.*, 4th Ser. **1979**, *47*, 311–348.

(16) (a) Osaka, T.; Nagasaka, H.; Goto, F. *J. Electrochem Soc.* **1980**, *127*, 2343–2346. (b) Horkans, J.; Kim, J.; McGrath, C.; Romankiw, L. T. *J. Electrochem Soc.* **1987**, *134*, 300–304.

(17) Shipley's literature on Niposit 468 bath indicates that the bath deposit 99.5% pure nickel metal containing 0.25% boron. The deposited film has a resistivity of 18 μΩ/cm and is ferromagnetic.



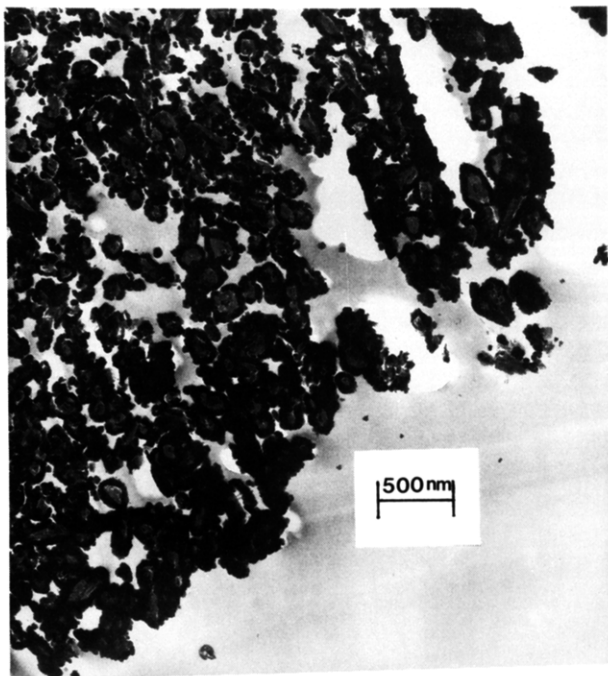


**Figure 7.** TEM micrograph of an ultrathin section of nickel-coated halloysite particles. Before sectioning the particles were embedded in an epoxy matrix. The darker areas represent metallic nickel. The lighter background is either the aluminosilicate layers of halloysite or the epoxy matrix.

in a fluid epoxy medium, aligning them with a magnetic field, and locking the alignment by curing the matrix in the magnetic field. An AFM picture of sections of such aligned composite is shown in Figure 6, revealing the parallel orientations of the metalized cylindrical halloysite particles.

A TEM micrograph of an ultrathin (30–40 nm) section of a composite containing embedded nickel-coated halloysite particles is shown in Figure 7. The darker circular regions represent the cross sections of nickel wrappings on the particles and therefore outline the particle diameter. (TEM examination of thin sections of epoxy composites containing embedded pristine halloysite particles failed to show any distinguishable contrast between the epoxy matrix and the halloysite particles and therefore could not image the cross sections of pristine halloysite particles.) From Figure 7, the halloysite tubes appear to vary in diameter and degree of roundness. Some tubes appear to be polyhedral rather than circular in cross section. These distortions from the circular geometry may however be an artifact from the microtoming process. Ceramic materials are known to be brittle and do not cut with a diamond blade without a considerable degree of fracture. From the width of the dark regions in Figure 7, the average thickness of the nickel film on halloysite particles has been calculated to be about 20 nm. Evidence of any nickel deposition on the inside surface of the halloysite particles was not seen in Figure 7, except a tiny inner central dark spot in some of the cross sections. (We are not sure whether these tiny central dots represent some metal depositions at the hollow inner core of the halloysite particles.) Considering the open ended and hollow nature of these particles as revealed from the AFM micrograph (Figure 3), the lack of metal deposition on the inside surface of halloysite can be attributed either to an inadequate catalyzation of the inside surface by the stannous chloride–palladium chloride treatment or to an inadequate degree

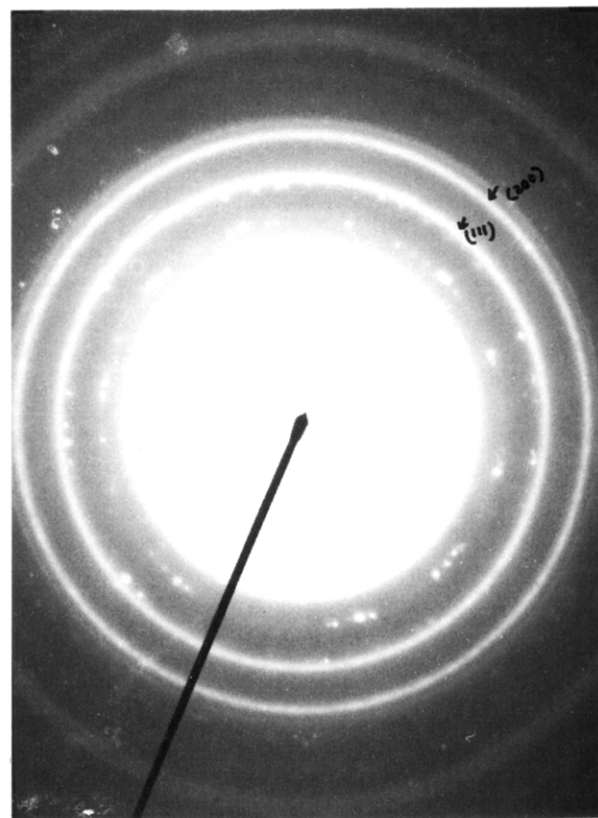


**Figure 8.** Selected area electron diffraction pattern recorded from the ultrathin section shown in Figure 7. The rings originating from the microcrystalline nickel particles are indicated by arrows and indexed as (111) and (200) respectively (outward from center).

of diffusion of chemicals to the inside surface of the particles during catalyzation and plating. The latter seems unlikely considering that the inside diameters of these particles are about 40 nm (Figure 3), which should be sufficiently large to allow adequate diffusion. [It appears from the TEM micrographs (Figure 7) that considerable diffusion of epoxy material inside the nickel-coated halloysite particles have taken place during the embedding step of the sample preparation.] We believe that the nature of the inside surface in halloysite particles may be different from that of the outer surface.

A selected area electron diffraction pattern from the cross section of coated particles is shown in Figure 8. The broad rings, marked in Figure 8 with arrows, have been indexed as 111 and 200 reflections of nickel metal with a face centered cubic (fcc) crystal structure. The broad diffraction rings from the nickel film indicate the metal to be microcrystalline.

The presence of microcrystalline nickel metal with an fcc structure is also indicated from X-ray powder diffraction pattern of nickel coated halloysite as shown in Figure 3b. Comparison of the powder diffraction patterns of halloysite before and after nickel coating indicates that the position of the peaks originating from the aluminosilicate framework of halloysite remained unchanged. The absence of any increase in the interlayer separation (indicated by no detectable shift in (001) and (002) peaks of halloysite) strongly suggests that intercalation of nickel metal or any other material within the rolled aluminosilicate layers of halloysite particles did not occur during metalization. The average grain size of the nickel microcrystallites has been calculated from the line width of

the (111) peak of nickel to be 4 nm by applying the Debye-Scherrer equation.<sup>18</sup> The intensity distribution of various peaks of nickel metal and halloysite did not alter significantly when the nickel-coated halloysite particles were oriented with a magnetic field before recording the diffraction pattern.

The thermogravimetric curve of the nickel coated halloysite is very similar (Figure 4b) to that of pristine halloysite particles (Figure 4a), except that the degree of weight loss is reduced particularly below 150 °C. The large decrease in weight loss below 150 °C observed with metalized halloysite may be due to replacement of water of hydration by acetone during storage of the metalized halloysite under acetone. Almost all of this acetone escapes during drying. A control experiment with pristine halloysite kept under acetone for 3 days also showed very little weight loss below 150 °C. The reduction in the observed weight loss between 390 and 525 °C (5.5% instead of 10% for pristine halloysite) is in accord with the presence of the 35–45 wt % of nickel (as determined from the chemical analysis of the coated halloysite particles). The nickel coat remains unchanged during heating in nitrogen atmosphere. Using the density of bulk nickel (8.9 g/cm<sup>3</sup>) for the nickel film, an average film thickness of about 10 nm was calculated for the nickel coating on halloysite (using both the weight loss and the chemical analysis data). The film thickness obtained from the TEM micrographs (Figure 7) of the particle cross sections is on the other hand about 20 nm, indicating that the deposited nickel film is probably considerably less dense than bulk nickel. The low density of the nickel coating is probably indicative of porous nature of the as-deposited nickel film. This may be caused by entrapment of hydrogen gas evolved during electroless metalization.

### Conclusions and Implications

We have demonstrated that cylindrical halloysite particles of approximately 1- $\mu$ m length and 100-nm diameter can be coated to a thickness of about 20 nm with microcrystalline films of ferromagnetic nickel metal. The purification and coating processes do not alter the particle morphology. There are many potential applications of

this type of metalized ceramic particles. For example, the ductility and toughness of ceramic materials obtained from halloysite clay may improve by using metalized halloysite instead. Numerous studies have shown that improved fracture toughness can be achieved by the incorporation of a ductile second phase into a brittle matrix.<sup>19</sup> The metalized particles can also be dispersed randomly or magnetically oriented in a ceramic, a metallic, or an organic polymer matrix to produce novel composite materials for dielectric, magnetic, and microwave applications. The halloysite particles can act as reinforcing component in ceramic composites, being weakly bound to the matrix due to the presence of metal interphase at the ceramic-ceramic junction.<sup>20</sup> On the other hand, the metal cladding may permit stronger bonding with the matrix in a metal matrix composite. The particles may also be utilized in sensor applications to detect a threshold level of strain or friction in a mechanical system. For example, by placing an indicator material such as a fluorescent dye in the core, strain or cracks in the tube may be detected by diffusion of the indicator material in the surrounding medium. Furthermore it may be possible to control the threshold detectable strain by controlling the strength of the metal coating (thickness, different metals, etc.) or by intercalation of materials into the halloysite layer structure. Wearing of a surface to a critical depth can also be sensed by incorporating halloysite containing indicator at a particular point in the composite material. We are at present exploring these potential applications of metalized halloysite particles.

**Acknowledgment.** We are grateful to Gan Moog Chow and Ron Price (for electron microscopy) and to Sayed Qadri (for X-ray powder diffraction). We sincerely acknowledge helpful suggestions from Paul Schoen. Financial support from the Office of Naval Technology is gratefully acknowledged.

(19) (a) Rankin, D. T. *J. Am. Ceram. Soc.* 1971, 54, 277–281. (b) Kristie, V. V.; Nicholisin, P. S. *J. Am. Ceram. Soc.* 1981, 64, 499–504. (c) Shaw, M. C.; Marshall, D. B.; Evans, A. G. *Proc. Mater. Res. Soc. Symp.* 1990, 170, 25–31. (d) Xiao, L. *Developments in Ceramic and Metal-Matrix Composites*; Upadhyay, K., Ed.; The Minerals, Metals and Materials Society, 1991; pp 115–124.

(20) Shimansky, R. A.; Hahn, H. T.; Salamon, N. J. *Proc. Mater. Res. Soc. Symp.* 1990, 170, 193–204.

(18) Taylor, A. *X-ray Metallography*; Wiley: New York, 1983; pp 674–685.